Exceptional service in the national interest

Sandia National Laboratories

SAND2015-2467PE

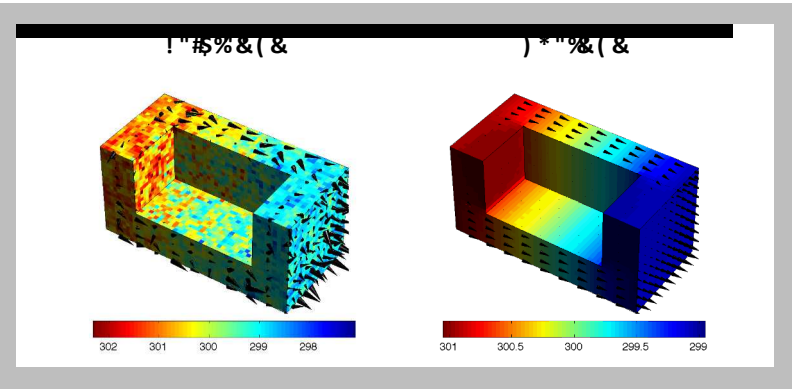

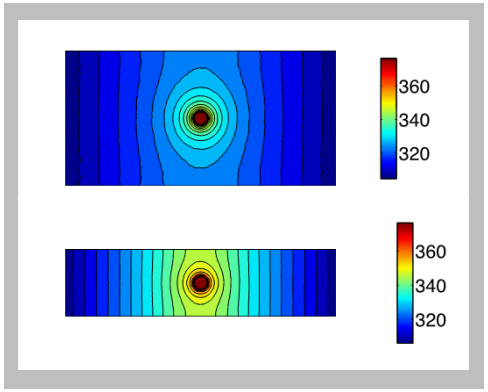

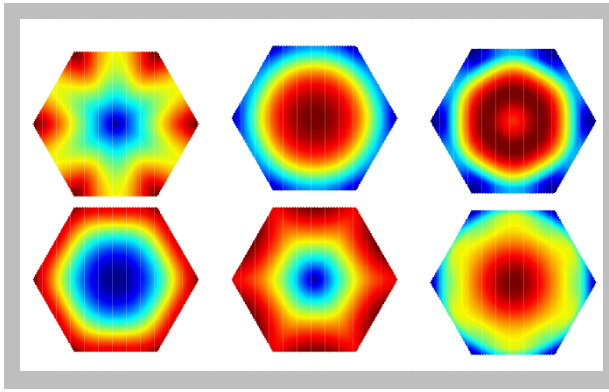

Monte Carlo Simulations of the Boltzmann-Peierls Equation

Colin Landon

U.S. DEPARTMENT OF ENERGY

National Nuclear Security Administration

Sandia National Laboratories is a multi-program laboratory managed and operated by Sandia Corporation, a wholly owned subsidiary of Lockheed Martin Corporation, for the U.S. Department of Energy's National Nuclear Security Administration under contract DE-AC04-94AL85000. SAND NO. 2011-XXXXP

Nanoscale

- Atomistic Simulation (i.e. Molecular Dynamics)
- Capture the physics of defects, surfaces, relaxation times, dispersion relations, etc.
- Limited in length and time scales

Ab inito

Mesoscale

- Simulation of Boltzmann Transport Equation (e.g. Monte Carlo, Lattice Boltzmann)
- Phonon relaxation times and dispersion relation must be known

Dispersion relation
Scattering rate (pathways)

Macroscale

- Fourier's law is typically valid when the phonon mean free path (O(100 nm) in silicon at 300K) is much smaller than the characteristic length scale of the problem

When Fourier's Law Fails

- Thermal energy is carried by atomic vibrations.
- Semi classical view: phonon (both wave and particle)
- Graphene phonon mean free path:

$$\Lambda \approx 600\text{nm}^{\dagger}$$

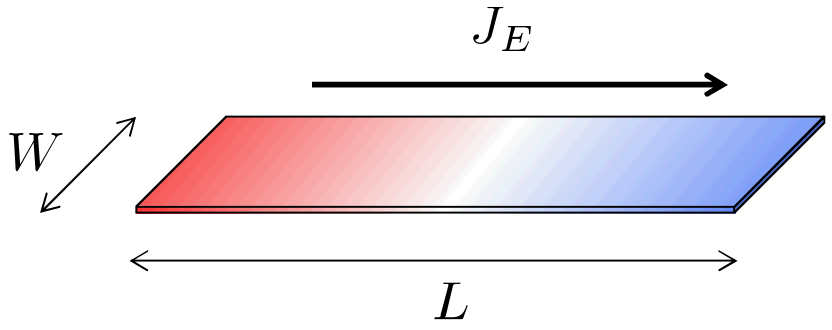

- Transport regimes
  - Diffusive $Kn \lesssim 0.1$
  - Transition $0.1 \lesssim Kn \lesssim 10$
  - Ballistic $Kn \gtrsim 10$

$$Kn_L = \Lambda/L \qquad Kn_W = \Lambda/W$$

$$J_E \neq \kappa \frac{dT}{dx}$$

†Pop, E., Varshney, V., and Roy, A. K., *MRS Bulletin*, 37, 1273–1281 (2012).

Boltzmann-Peierls Equation (BPE)

Sandia National Laboratories

- Thermal transport is balance of advection and scattering

$$\frac{\partial n(\mathbf{x},\mathbf{q},s,t)}{\partial t} + \mathbf{v}(\mathbf{q},s)\cdot\nabla_{\mathbf{x}} n(\mathbf{x},\mathbf{q},s,t) = \left[\frac{\partial n(\mathbf{x},\mathbf{q},s,t)}{\partial t}\right]_{\text{scatt}}$$

$$= \sum_{\mathbf{q}'s',\mathbf{q}''s''} \left[\left(P^{\mathbf{q}s,\mathbf{q}'s'}_{\mathbf{q}''s''} - P^{\mathbf{q}''s''}_{\mathbf{q}s,\mathbf{q}'s'}\right) + \frac{1}{2}\left(P^{\mathbf{q}s}_{\mathbf{q}'s',\mathbf{q}''s''} - P^{\mathbf{q}'s',\mathbf{q}''s''}_{\mathbf{q}s}\right)\right]$$

- Challenges for modeling BPE:
  - High dimensionality (3 spatial, 3 velocity, time)
  - Discontinuities
  - Complicated scattering model

$$P^{\mathbf{q}''s''}_{\mathbf{q}s,\mathbf{q}'s'} = \frac{2\pi}{\hbar^2}|\tilde{\mathcal{V}}_3(-\mathbf{q}s,-\mathbf{q}'s',\mathbf{q}''s'')|^2 n(\mathbf{q}s)n(\mathbf{q}'s')(n(\mathbf{q}''s'')+1)$$
$$\times\delta(-\omega(\mathbf{q}s)-\omega(\mathbf{q}'s')+\omega(\mathbf{q}''s''))\delta(-\mathbf{q}-\mathbf{q}'+\mathbf{q}''+\boldsymbol{G})$$

Simplification of BPE

- Relaxation time approximation

$$\left[\frac{\partial n}{\partial t}\right]_{\text{scatt}} = -\frac{n - n^{\text{eq}}}{\tau}$$

$$n^{\text{eq}} = \frac{1}{\exp(\hbar\omega/k_{\text{B}}T) - 1}$$

ANALYSIS OF LATTICE T

A fit of the data on high purity silicon using the Callaway equation is shown in Fig. 2. The experimental data are taken from Holland and Neuringer[12] (1.7 to 300°K), and Slack and Glassbrenner[40] (300 to 1683°K). The two sets of data agree within two percent at room temperature. A fit at high temperature, obtained from Eq. (8), is also shown. The value of (D_1+D_2) is obtained from the 1000°K data using Eq. (18).

In Fig. 3, the same silicon data are fit using the new formulation. Each contribution is shown. The value of κ_{TU} is obtained from the 1000°K data using Eq. (17b). κ_L is then obtained from the data near room temperature with the value of κ_{TU} taken into account. κ_{T0} will be insignificant at 300°K. κ_{T0} is then obtained from the best fit for the low-temperature data with κ_{TU} and κ_L taken into account. This procedure may seem somewhat

- Analytical decomposition†† (not linearization)

$$n = n^{\text{d}} + n^{\text{eq}}$$

$$\frac{\partial n^{\text{d}}}{\partial t} + \mathbf{v}(\mathbf{q}, s) \cdot \nabla_{\mathbf{x}} n^{\text{d}} = \left[\frac{\partial n^{\text{d}}}{\partial t}\right]_{\text{scatt}}$$

- Energy Boltzmann†††

$$f = \hbar\omega n$$

$$\frac{\partial f}{\partial t} + \mathbf{v}(\mathbf{q}, s) \cdot \nabla_{\mathbf{x}} f = \left[\frac{\partial f}{\partial t}\right]_{\text{scatt}}$$

† Holland, M.G., *Phys. Rev.*, **132**, 2461–2471 (1963).
†† Baker, L. L. and Hadjiconstantinou, N. G., *Phys. Fluids*, **17**, 051703 (2005).
††† Péraud, J.-P. M. and Hadjiconstantinou, N. G., *Phys. Rev. B*, **84**, 205331 (2011).

Monte Carlo Simulation of BPE

$$\underbrace{\frac{\partial n}{\partial t} + \mathbf{v}(\mathbf{q}, s) \cdot \nabla_{\mathbf{x}} n}_{\text{Advection}} = \left[\frac{\partial n}{\partial t}\right]_{\text{scatt}}$$

- Not limited to relaxation time approximation
- Particle representation of distribution function, "phonons"

$$n(\mathbf{x}, \mathbf{q}, s, t) \approx N_{\text{eff}} \sum \delta(x - x_i(t))\delta(q - q_i)\delta_{s,s_i}$$

- Time splitting: advect then collide
- Stochastic sampling—heat flux in cell m:

$$\mathbf{J}_m = N_{\text{eff}} \sum_{\{i|x_i \in m\}} \hbar\omega(\mathbf{q}_i, s)\mathbf{v}(\mathbf{q}_i, s)$$

$$\sigma(J_M) \propto 1/\sqrt{N_m}$$

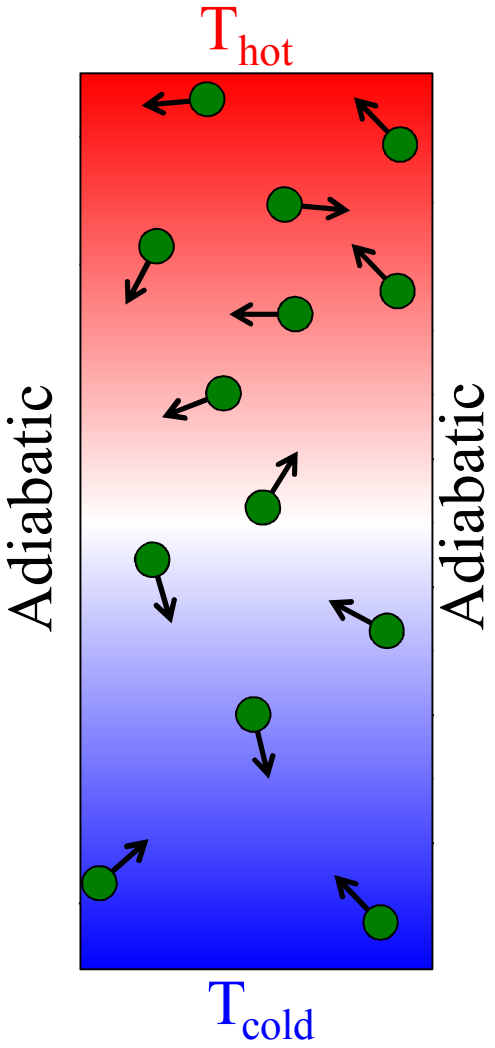

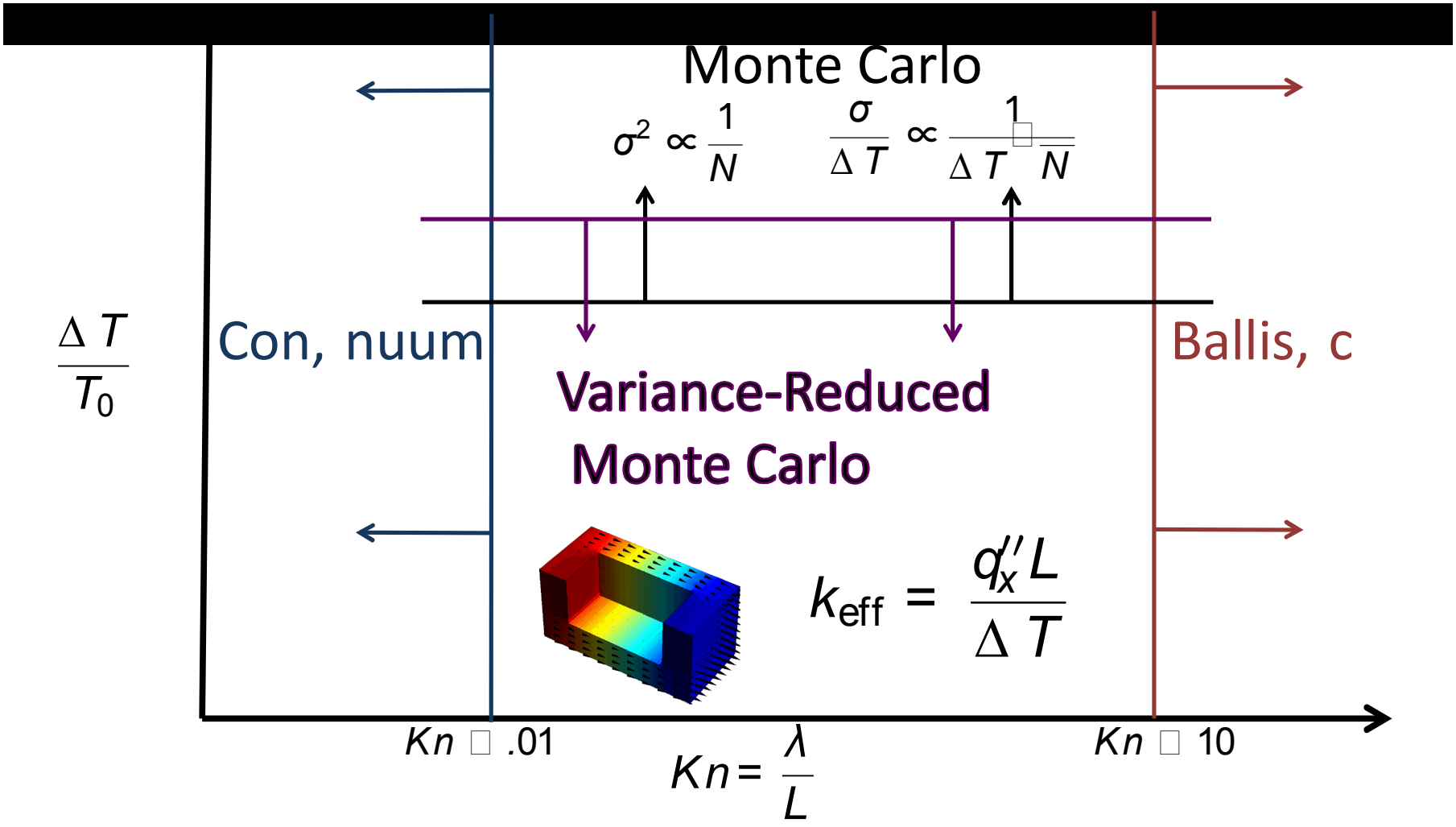

Lambda/L

Je instead of qx

Variance Reduction for BPE

- Analytic decomposition and energy BPE

$$f^{\mathrm{d}} = \hbar\omega n - \hbar\omega n^{\mathrm{eq}}$$

- Particles now represent deviational energy

$$f^{\mathrm{d}}(\mathbf{x}, \mathbf{q}, s, t) \approx \sum_i E_{\mathrm{eff}} \sigma_i \delta(\mathbf{x} - \mathbf{x}_i(t)) \delta(\mathbf{q} - \mathbf{q}_i) \delta_{s,s_i}$$

- Sampling consists of stochastic part and analytic part—energy density in cell m:

$$u_m = \underbrace{u_m^{\mathrm{d}}}_{\text{noisy}} + \underbrace{u^{\mathrm{eq}}}_{\text{exact}}$$

$$u_m = \frac{\sum_{\{i|\mathbf{x}_i \in \text{cell } m\}} E_{\mathrm{eff}} \sigma_j}{V_{\mathrm{cell}}} + u^{\mathrm{eq}}$$

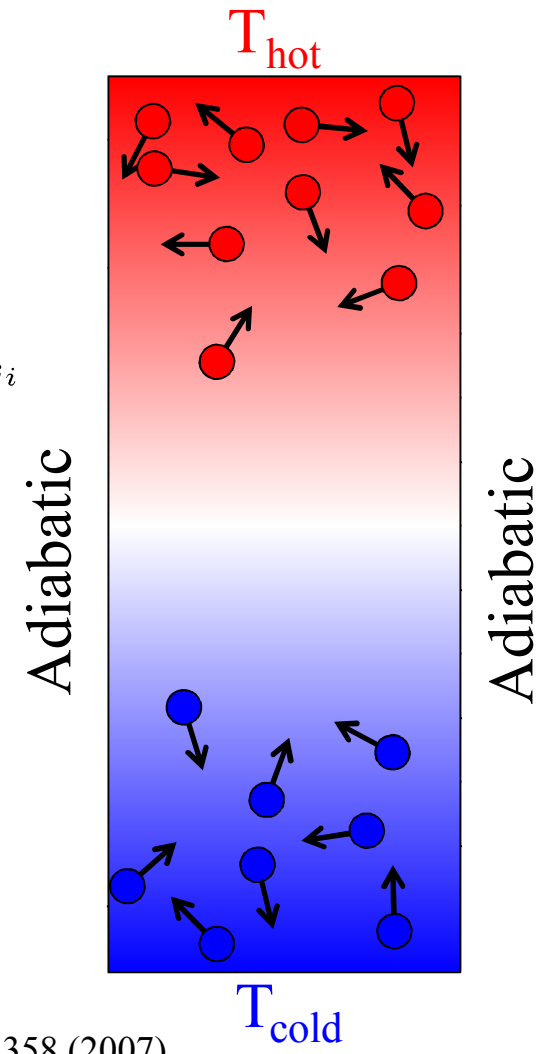

Low Variance Deviational Simulation Monte Carlo (LVDSMC):
Baker, L. L. & Hadjiconstantinou, N. G. *Phys. Fluids*, **17**, 051703 (2005).
Homolle, T. M. M. & Hadjiconstantinou, N. G. *J. Comput. Phys.*, **226**, 2341-2358 (2007).
Péraud, J.-P. M. and Hadjiconstantinou, N. G. *Phys. Rev. B*, **84**, 205331 (2011).

Variance Reduction Example 1: Line heating

- 10 nm line heating semi-infinite silicon domain
- Automatic and intelligent focusing of computational effort
- Areas at equilibrium are simulated exactly with no computational cost

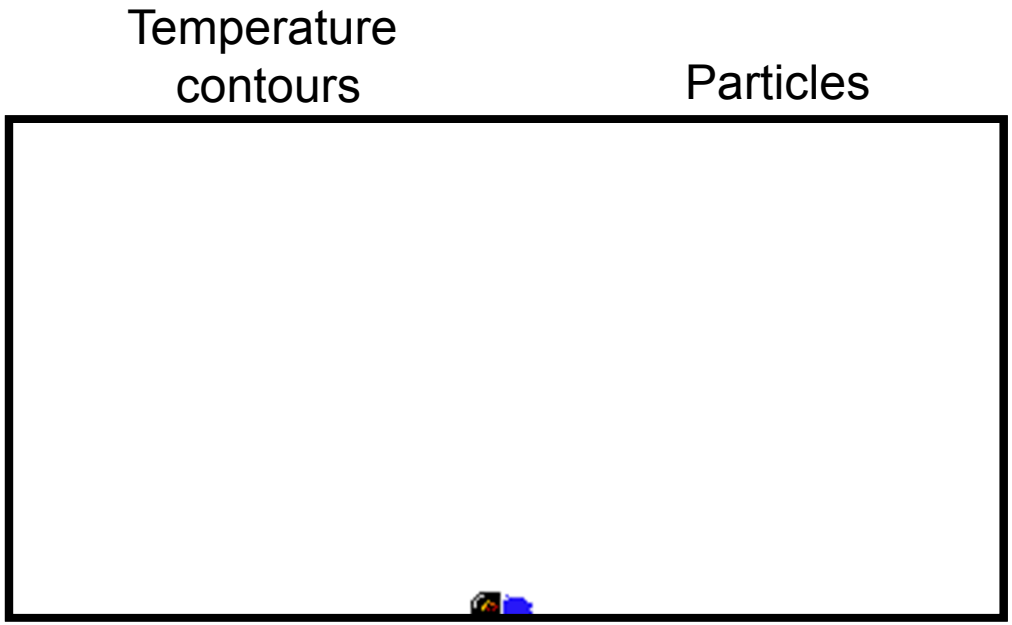

Variance Reduction Example 2: Silicon Nanopore (Temperature Field)

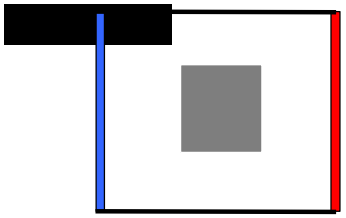

Structure is spa, ally periodic

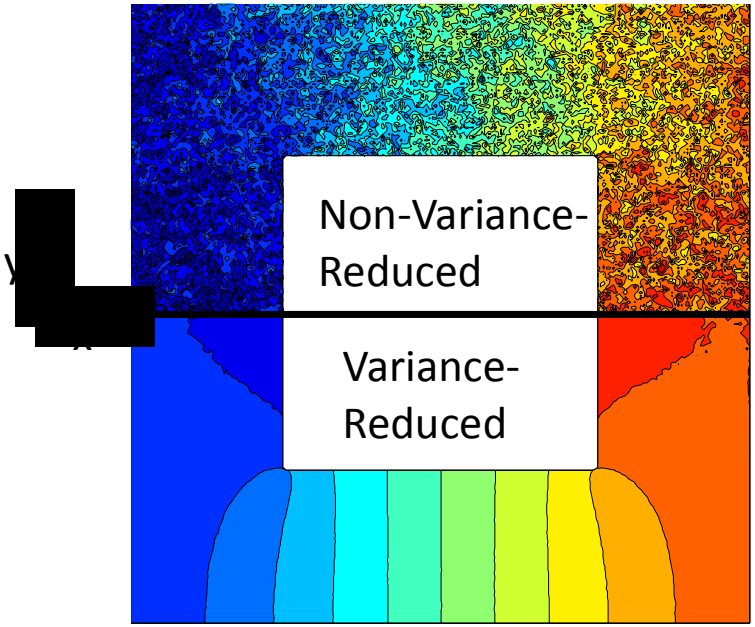

130 nm Kn = .97

Simulation run time (both): ~2.5 days on 3.0 GHz processor

To get the non-VR simula, on to the same resolu, on would take **60+ years**

Variance Reduction Example 2: Silicon Nanopore (Heat Flux)

Sandia National Laboratories

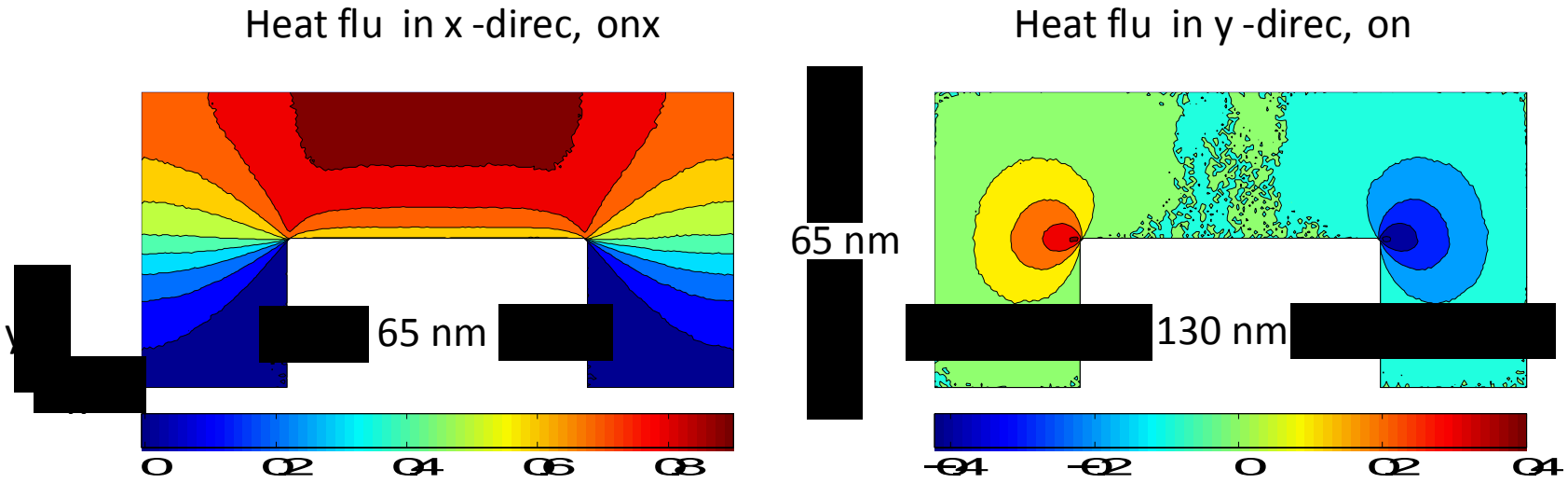

Simulation run time:
~2.5 days on 3.0 GHz processor

* Periodic structure in x-direc, on

**Heatx flu normalized by bulk heat flu

To get the standard simula, on to the same resolu, on would take **60+ years**

Relaxation Time Approximation and Graphene

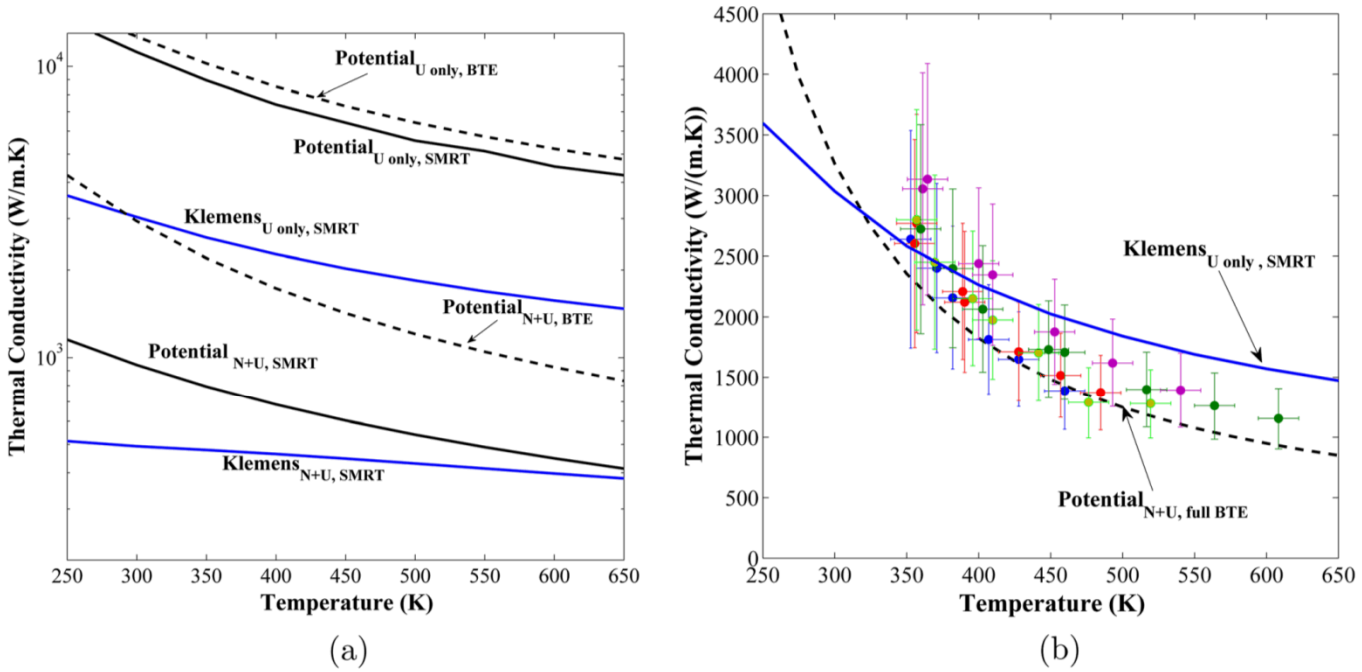

FIG. 5. (Color online) Thermal conductivity variation with temperature. (a) The different curves are labeled in accordance with the corresponding approximation employed. The dotted lines correspond to values obtained from the solution of the phonon BTE while the solid lines denote thermal conductivity computations performed under the single mode relaxation time approximation. (b) Comparison of computed thermal conductivity with experimental data.

- Single mode relaxation time (with either phenomenonlogical rates or ab-initio calculated rates) dramatically under-predicts thermal conductivity

Beyond the Relaxation Time Approximation

Ab Initio thermal transport

- Analytical decomposition, energy BPE, spatially homogeneous, time independent, 1d temperature gradient (dT/dx), linearize RHS

$$\frac{\partial f_\lambda^{\mathrm{eq}}}{\partial T}\frac{\mathrm{d}T}{\mathrm{d}x} = \frac{A_{\mathrm{uc}}}{2\pi\hbar^2}\sum_{s',s''}\int \mathrm{d}^2\mathbf{q}'|\tilde{\mathcal{V}}_3(-\lambda,-\lambda',\lambda'')|^2\delta(-\omega_\lambda-\omega_{\lambda'}+\omega_{\lambda''})$$
$$\times\left((f^0_{\lambda''}-f^0_{\lambda'})f^{\mathrm{d}}_\lambda+(f^0_{\lambda''}-f^0_\lambda)f^{\mathrm{d}}_{\lambda'}+(f^0_\lambda+f^0_{\lambda'}+1)f^{\mathrm{d}}_{\lambda''}\right)$$
$$+\frac{A_{\mathrm{uc}}}{4\pi\hbar^2}\sum_{s',s''}\int \mathrm{d}^2\mathbf{q}'|\tilde{\mathcal{V}}_3(-\lambda,\lambda',\lambda'')|^2\delta(-\omega_\lambda+\omega_{\lambda'}+\omega_{\lambda''})$$
$$\times\left(-(f^0_{\lambda''}+f^0_{\lambda'}+1)f^{\mathrm{d}}_\lambda+(f^0_{\lambda''}-f^0_\lambda)f^{\mathrm{d}}_{\lambda'}+(f^0_{\lambda'}-f^0_\lambda)f^{\mathrm{d}}_{\lambda''}\right)$$

where $(\mathbf{q},s)\to\lambda$, $\mathbf{q}+\mathbf{q}'=\mathbf{q}''+\mathbf{G}$ for first term and $\mathbf{q}=\mathbf{q}'+\mathbf{q}''+\mathbf{G}$ for second term

Anharmonic interaction term

- Fo

This is by far the biggest computational expense

It is made managable by:

1) Calculating the force constants from the atomistic simulation beforehand

2) Discretizing wavevector space to allow a finite number of interaction

3) Tabulating the interaction term for all allowable interactions at the beginning of a run

*NOTE: enforced symmetrization leads to changes of 20% in transport properties

$\tilde{V}_3(\mathbf{q}s$

$\Big)^{1/2}$

$\mathbf{q}''\mathbf{b}'')$

Brillouin Zone Discretization (2D)

- Discretization chosen so that momentum conservation is exactly satisfied on grid points
- Energy conservation is achieved by regularizing the delta function (linear triangle method)
- The result is the BPE as a linear system of equations

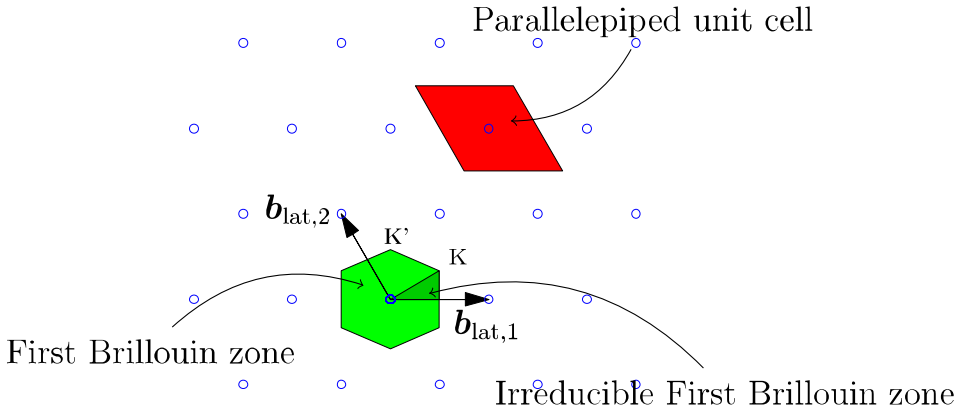

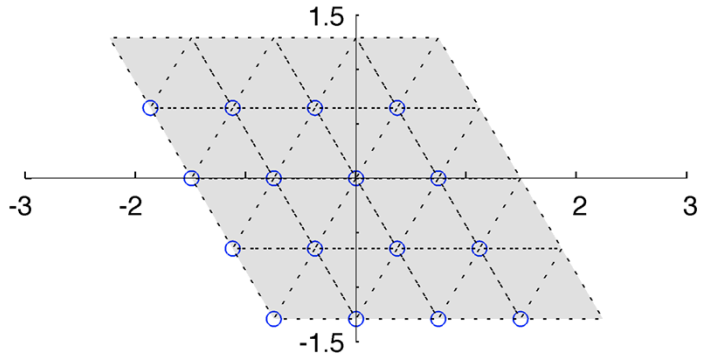

$$\mathbf{v}_i \cdot \nabla_{\mathbf{x}} f_i^{\text{eq}} = \sum_j B_{ij} f_j^{\text{d}}$$

Iterative Solution (Brief History)

Sandia National Laboratories

- 1995: Sparavigna formulated iterative solution
- 2003: Sparavigna published potential for silicon (2 & 3 body)
- 2004: Broido matches Si/Ge thermal conductivity (Keating model)
- 2005: Broido shows Tersoff and ED off by factor of 2, SW by factor of 4 for Si thermal conductivity
- 2007: Broido matches Si/Ge thermal conductivity with ab-initio calculations
- 2010: Lindsay and Broido use optimized Tersoff for graphene
- 2011: Singh shows failure of SMRT in graphene with Tersoff
- 2014: Lindsay uses ab-initio force constants for graphene

Map of a few relevant graphene simulations

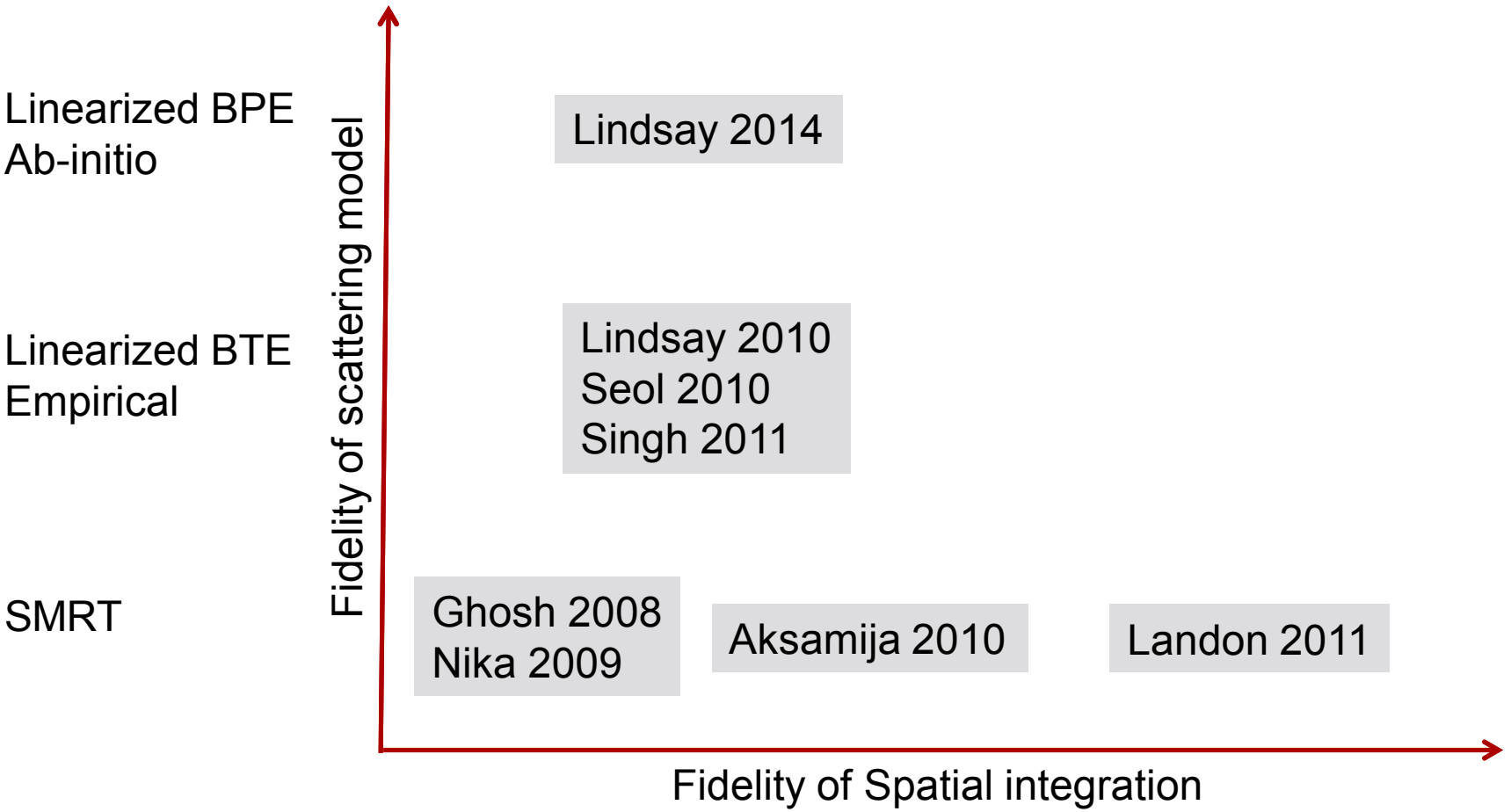

Linearized Ab Initio Phonon Low Variance Deviational Simulation Monte Carlo (LAIP-LVDSMC)

$$\frac{\partial f_i^{\mathrm{d}}}{\partial t} + \boldsymbol{v}_i \cdot \nabla_{\boldsymbol{x}} f_i^{\mathrm{d}} + \boldsymbol{v}_i \cdot \nabla_{\boldsymbol{x}} f_i^{0} = \sum_j B_{ij} f_j^{\mathrm{d}}$$

- How do you simulate the discrete deviational energy BPE with the matrix scattering operator?
  - LHS: Advection in MC
  - RHS: ???

LAIP-LVDSM Collision Operator

$$\left[\frac{\partial f_i^{\mathrm{d}}}{\partial t}\right]_{\mathrm{scatt}} = \sum_j B_{ij} f_j^{\mathrm{d}}$$

- Solution is analytic!

$$f_i^{\mathrm{d}}(t+\Delta t) = \sum_j P_{ij}(\Delta t) f_j^{\mathrm{d}}(t)$$

- Generator matrix

$$\boldsymbol{P}(\Delta t) = e^{\boldsymbol{B}\Delta t} = \sum_{k=0}^{\infty} \frac{\Delta t^k}{k!} \boldsymbol{B}^k$$

- Additional overhead, but minimal runtime cost

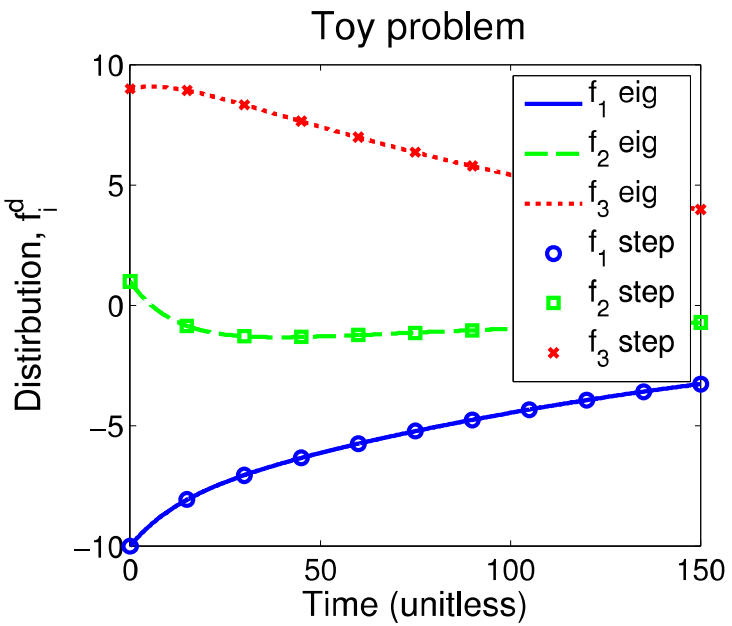

LAIP-LVDSMC Collision Algorithm

$$f_j^{\mathrm{d}}(t+\Delta t) = \sum_i \frac{P_{ji}(\Delta t)}{\mathcal{P}_i} \left(\sum_{n=0}^{\infty} \left(2\frac{\mathcal{P}_i^-}{\mathcal{P}_i} \right)^n \right) f_i^{\mathrm{d}}(t)$$

- Particle in state i, with sign σ
- Transition from i, to p with

$$\sum_{j=1}^{p-1} |P_{ji}| \leq \mathcal{R}\mathcal{P}_i < \sum_{j=1}^{p} |P_{ji}|$$

- Assign a new sign

$$\sigma' = \mathrm{sgn}(P_{pi}\sigma)$$

- If $\sigma' \neq \sigma$ generate 2 at i with sign σ
- Collision step is exact and energy conserving

Plot of Cumulant: $\sum_{j=1}^{p} |P_{ji}|$

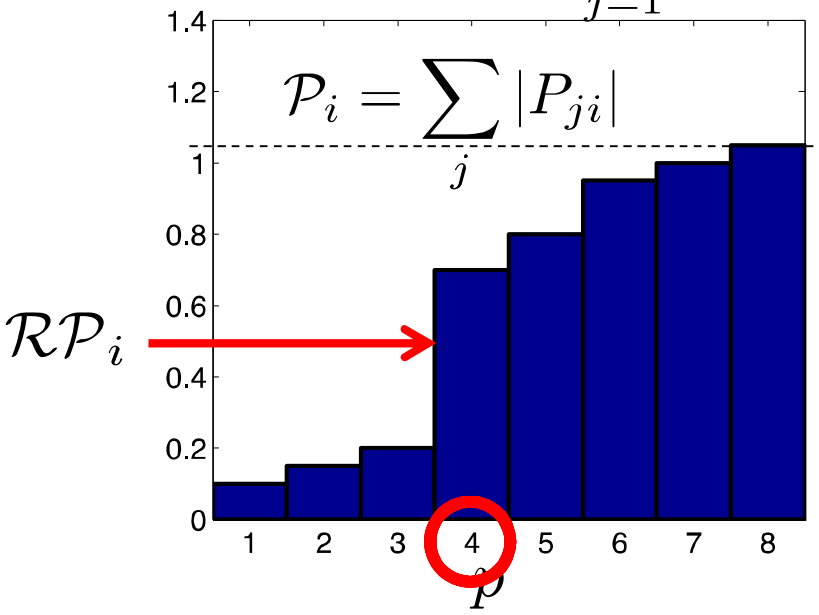

LAIP-LVDSM Algorithm

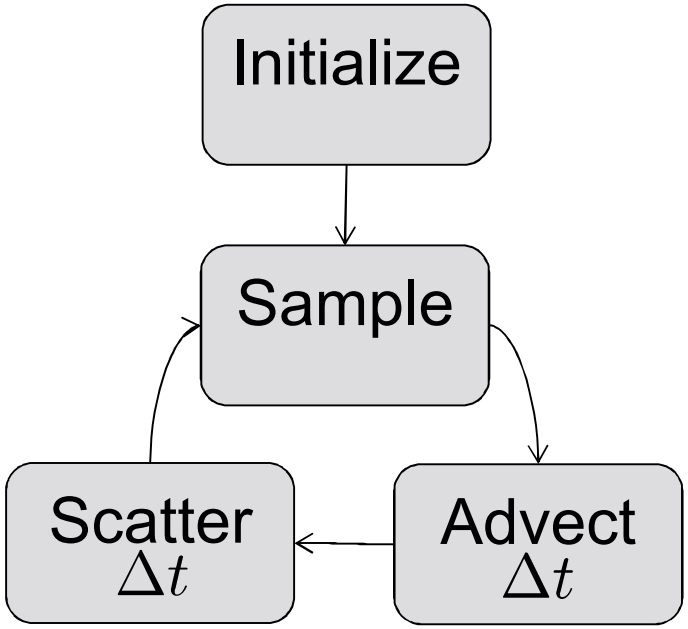

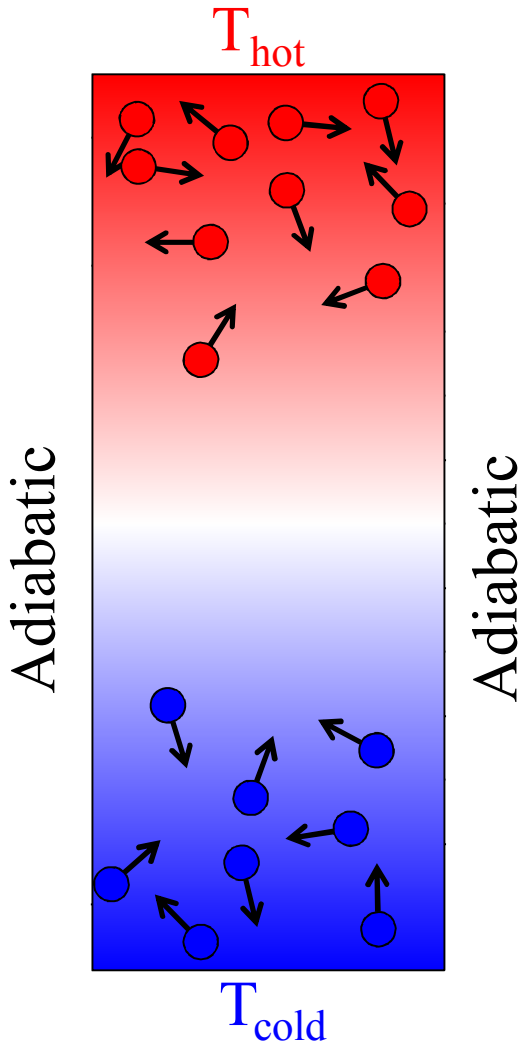

The devil is in the details (numerics)

- Anharmonic term is not properly symmetric

$$6|\tilde{V}_{3,\mathrm{sym}}(\lambda,\lambda',\lambda'')|^2 = |\tilde{V}_3(\lambda,\lambda',\lambda'')|^2 + |\tilde{V}_3(\lambda',\lambda,\lambda'')|^2 + |\tilde{V}_3(\lambda'',\lambda',\lambda)|^2 + |\tilde{V}_3(\lambda'',\lambda,\lambda')|^2 + |\tilde{V}_3(\lambda',\lambda'',\lambda)|^2 + |\tilde{V}_3(\lambda,\lambda'',\lambda')|^2.$$

- Transfer matrix, $\tilde{\mathbf{B}}$, does not describe momentum and energy conservation

$$\sum_i \tilde{B}_{ij} = \Delta_j \neq 0 \qquad \sum_i \frac{q_{x,i}}{\omega_i}\tilde{B}^{\mathrm{N}}_{ij} = \Delta^{\mathrm{N}}_{x,j} \neq 0 \qquad \sum_i \frac{q_{y,i}}{\omega_i}\tilde{B}^{\mathrm{N}}_{ij} = \Delta^{\mathrm{N}}_{y,j} \neq 0$$

Lagrange multiplier enforce conservation

$$B^{\mathrm{N}}_{ij} = \tilde{B}^{\mathrm{N}}_{ij} + \beta^{\mathrm{N}}_{ij}. \qquad 2\beta^{\mathrm{N}}_{ij} = -\lambda_j - \frac{q_{x,i}}{\omega_i}\lambda_{x,j} - \frac{q_{y,i}}{\omega_i}\lambda_{y,j}$$

$$\begin{bmatrix} \sum_i 1 & \sum_i \frac{q_{x,i}}{\omega_i} & \sum_i \frac{q_{y,i}}{\omega_i} \\ \sum_i \frac{q_{x,i}}{\omega_i} & \frac{\sum_i q^2_{x,i}}{\omega_i^2} & \sum_i \frac{q_{x,i}q_{y,i}}{\omega_i^2} \\ \sum_i \frac{q_{y,i}}{\omega_i} & \sum_i \frac{q_{x,i}q_{y,i}}{\omega_i^2} & \sum_i \frac{q^2_{y,i}}{\omega_i^2} \end{bmatrix} \begin{bmatrix} \lambda_j \\ \lambda_{x,j} \\ \lambda_{y,j} \end{bmatrix} = \begin{bmatrix} 2\Delta^{\mathrm{N}}_j \\ 2\Delta^{\mathrm{N}}_{x,j} \\ 2\Delta^{\mathrm{N}}_{y,j} \end{bmatrix}$$

Graphene Material Model

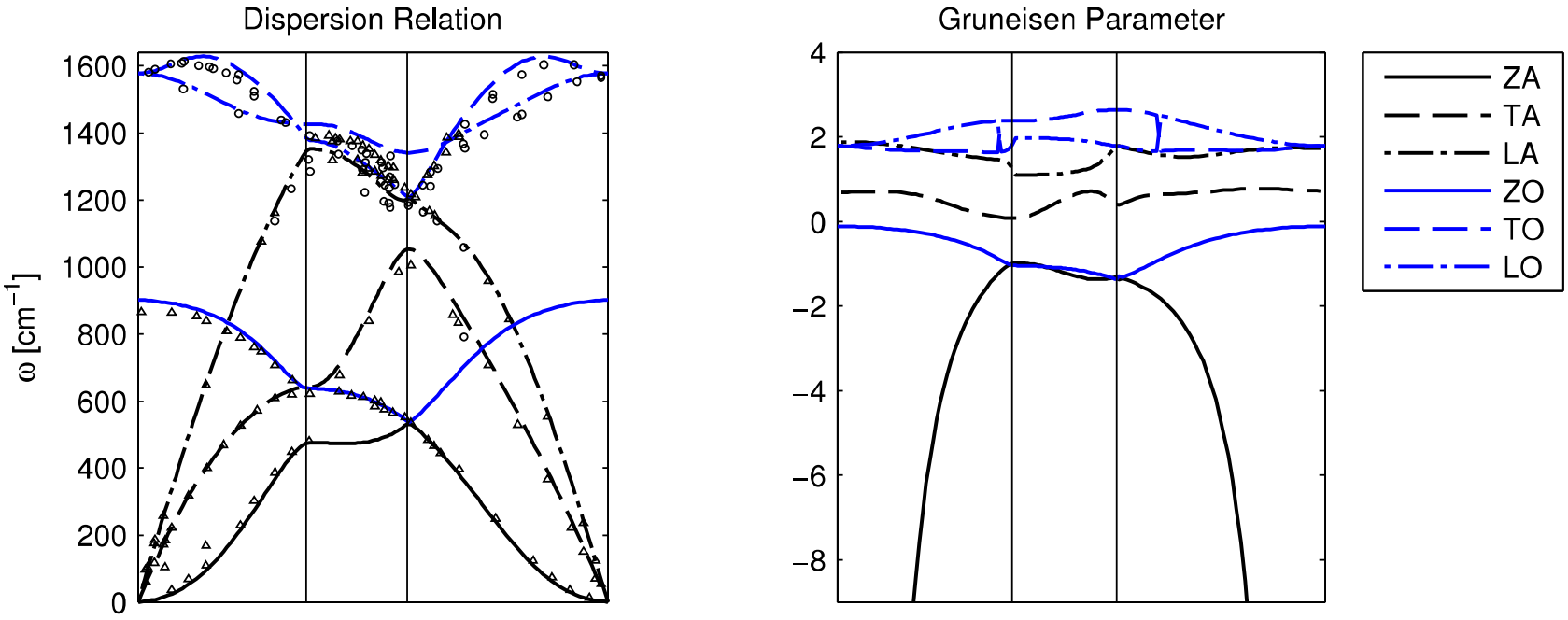

Circles: M. Mohr, et al., Phys. Rev. B 76, 035439 (2007).
Triangles: J. Maultzsch, et al., Phys. Rev. Lett. 92, 075501 (2004).

- Harmonic and anharmonic force constants from DFT/DFPT

Force constants used were calculated by Sangyeop Lee using code he and Keivan Esfarjani developed. See: Esfarjani, K. and Chen, G., *Phys. Rev. B*, **84,** 085204 (2011).

Validation: SMRT

$$\cancel{\frac{\partial f_i^{\mathrm{d}}}{\partial t}}^{\,0\ \text{Steady state}} + \boldsymbol{v}_i \cdot \nabla_{\boldsymbol{x}} f_i^{\mathrm{d}} + \boldsymbol{v}_i \cdot \nabla_{\boldsymbol{x}} f_i^{0} = B_{ij} f_j^{\mathrm{d}} \delta_{ij}$$

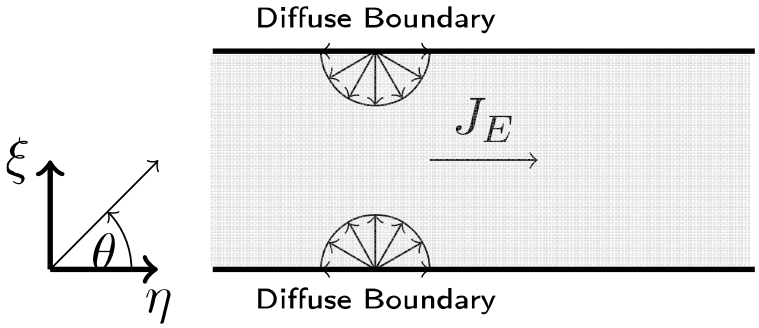

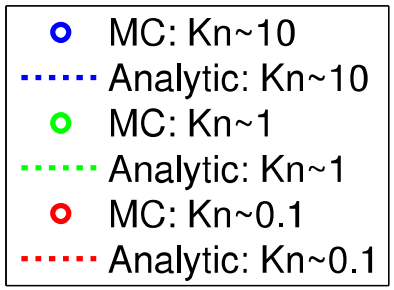

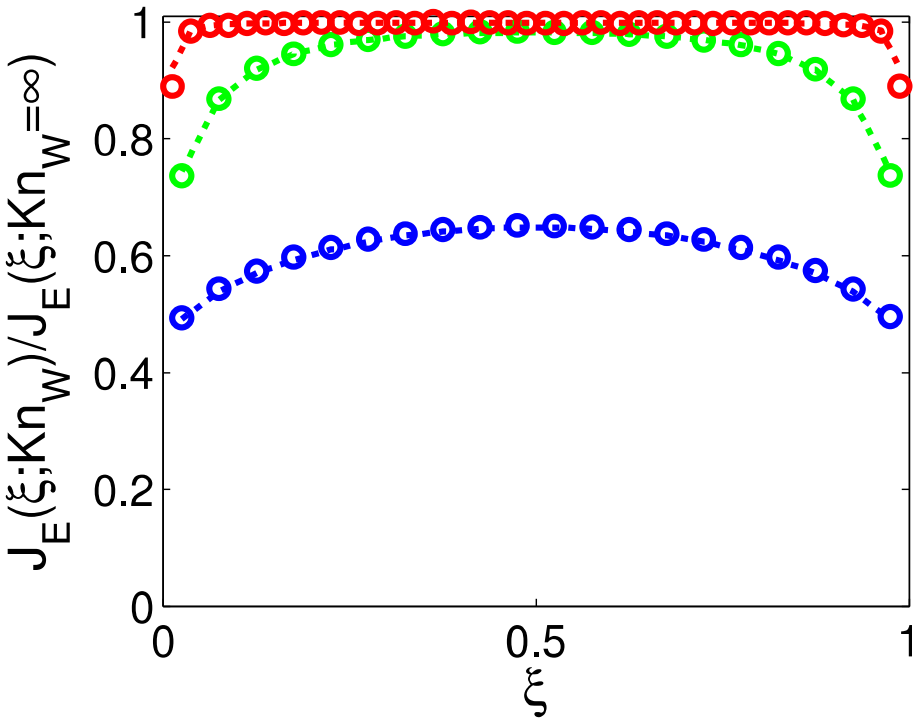

Validation: Homogeneous

$$\frac{\partial f_i^{\mathrm{d}}}{\partial t}^{0} + \boldsymbol{v}_i \cdot \nabla_{\boldsymbol{x}} f_i^{\mathrm{d}} + \boldsymbol{v}_i \cdot \nabla_{\boldsymbol{x}} f_i^{0}{}^{0} = \sum_j B_{ij} f_j^{\mathrm{d}} + 2\frac{v_i}{L_{\mathrm{b}}}$$

steady — homogenous — boundary

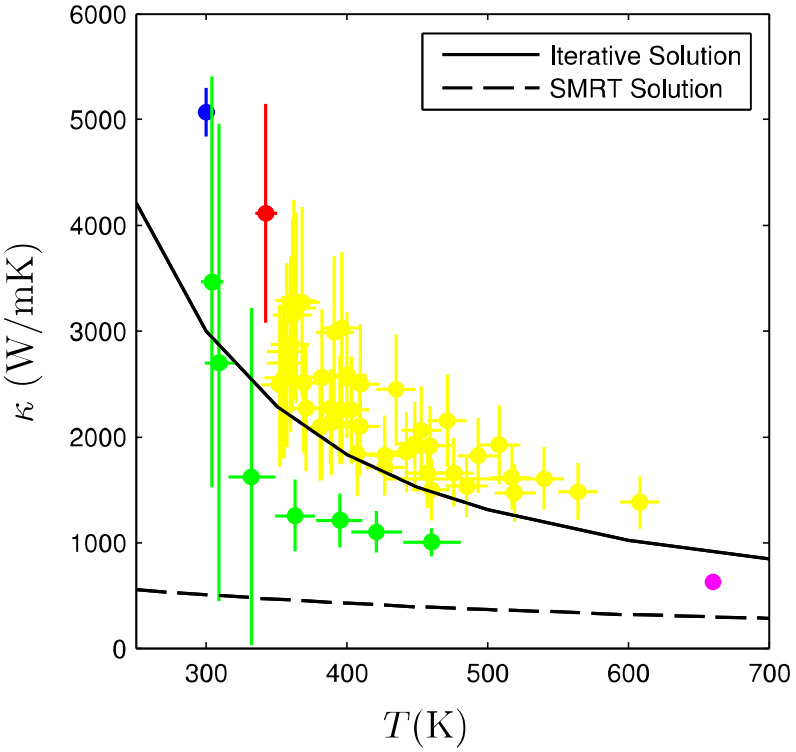

Model	κ (W/mK)	% ZA	% TA	% LA	% ZO	% TA	% LA
No Boundary Scattering	3600	86.1	9.10	2.47	2.37	-0.02	-0.02
Boundary (L_B=10 μm)	2999	83.1	10.8	3.57	2.63	-0.02	-0.02
Singh et al.	3216	88.9	7.53	2.85	0.007		
Lindsay et al.	3435	75.7	15.1	9.17			

References:

Lindsay, L., et al. Phys. Rev. B, 82, 115427 (2010)

Singh, D., *J. Appl. Phys.*, 110, 094312, (2011)

- Ghosh, S., et al. *Appl. Phys. Lett.*, 92, 151911 (2008)
- Balandin, A. A., et al. *Nano Lett.*, 89, 902–907 (2008)
- Chen, S., et al. *ACS Nano*, 5, 321–328 (2011)
- Lee, J.-U. et al. *Phys. Rev. B*, 83, 081419 (2011)
- Faugeras, C., et al. *ACS Nano*, 4, 1889–1892 (2010)

Study: Graphene Kinetic Size Effects

Sandia National Laboratories

Boundary Scattering

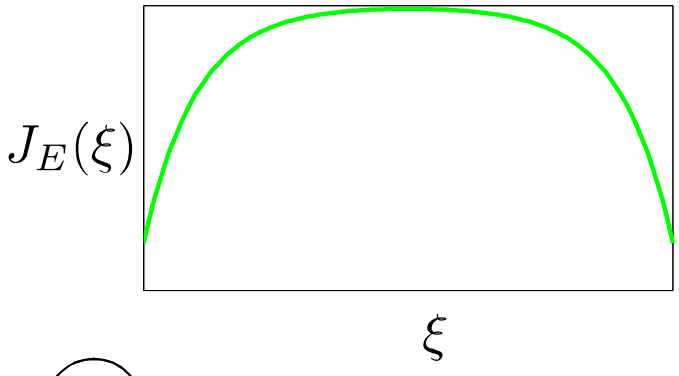

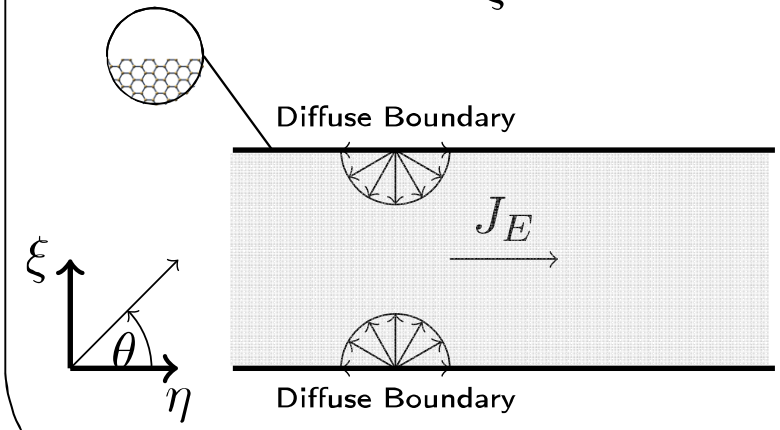

Temperature Jump

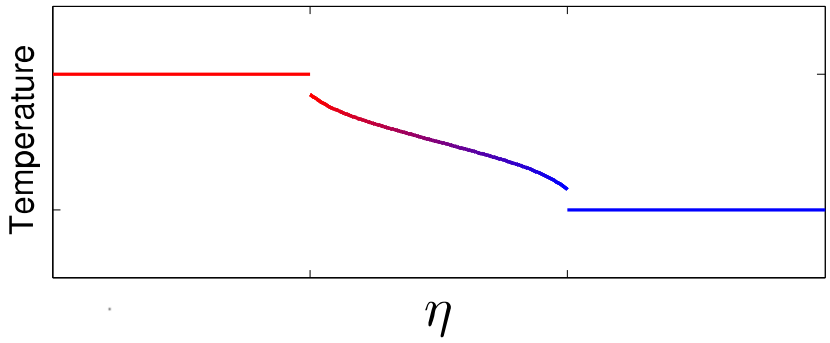

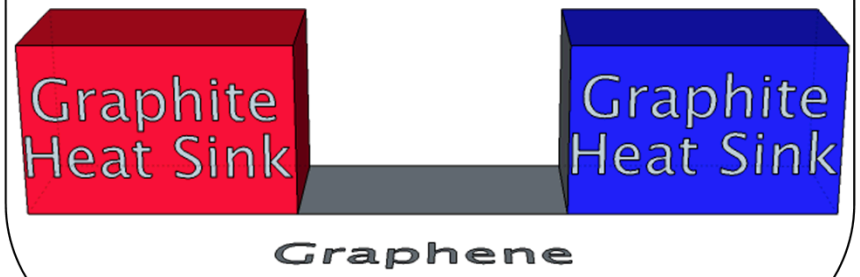

Finite Width Effects

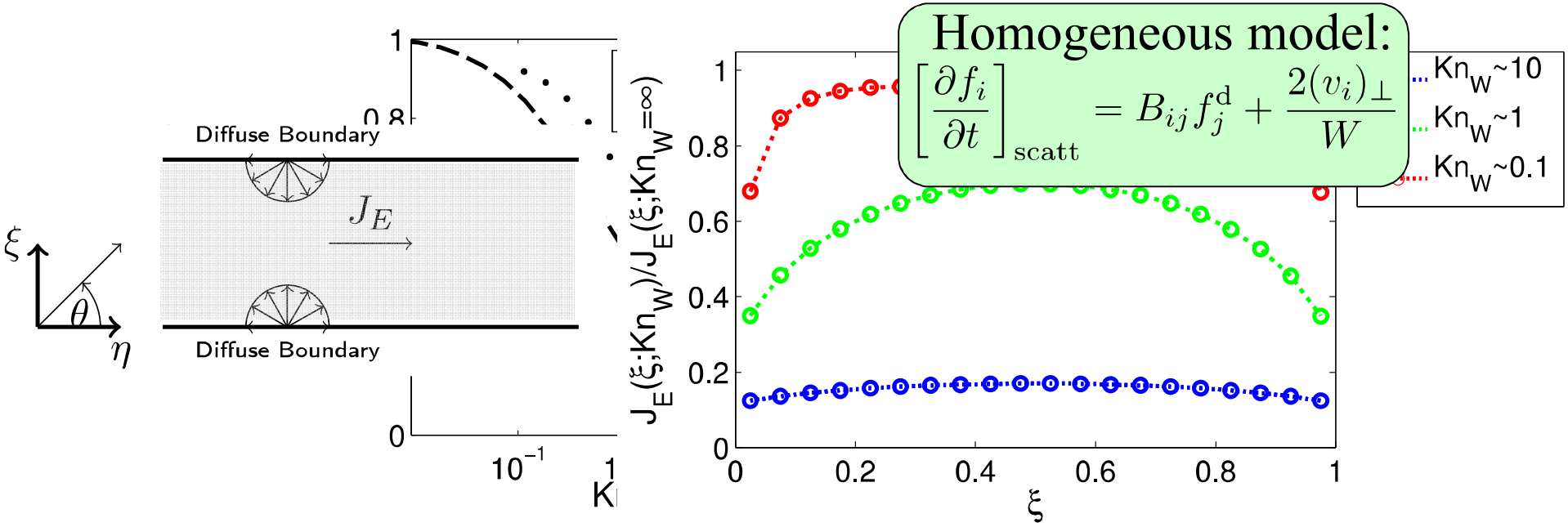

- Decreased transport region extends a few λ into the domain
- For 6 μm wide ribbons average transport is reduced by 10%
- Homogeneous scattering approximation introduces 10-30% error

Finite Length Effects

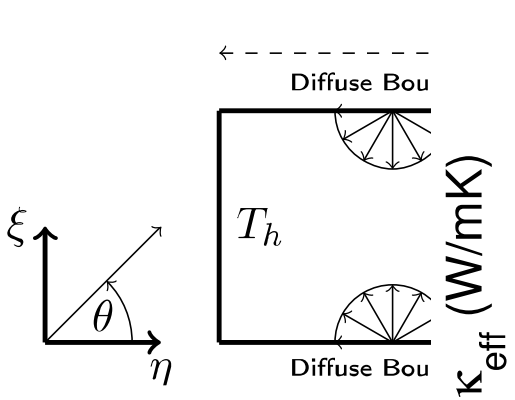

$$T^*(\eta) =$$

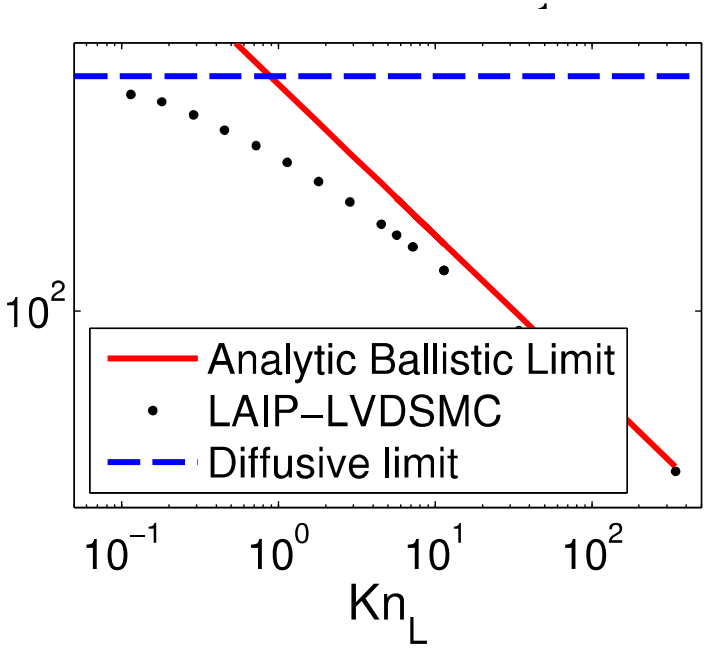

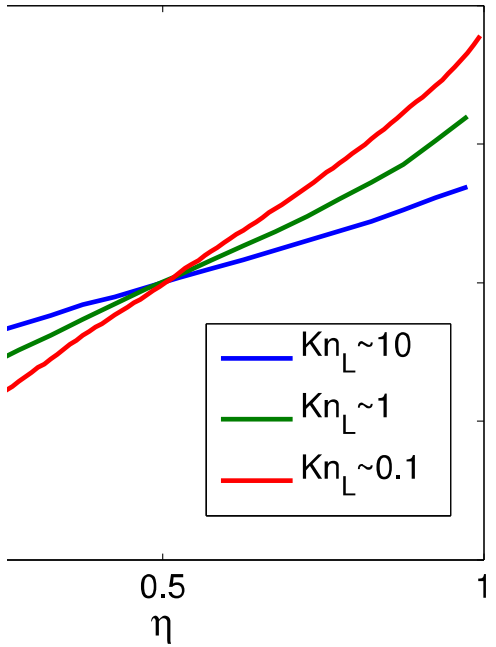

- Significant temperature jump for 6 µm long ribbons
- Knudsen layer extends a few mean free paths into the domain
- Agreement with diffusive and ballistic† limits

†Bae, M.-H., et al., Nat. Commun. 4, 1734 (2013).

2D Kinetic Size Effects

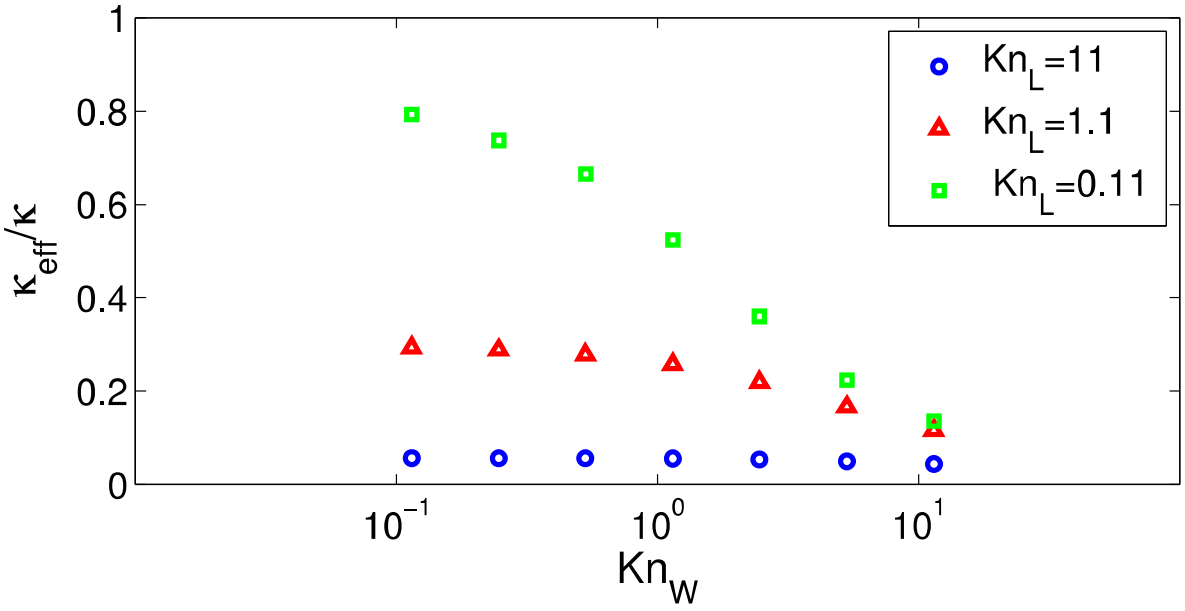

- First explicitly 2D simulation of graphene with ab-initio scattering
- Simulation stats: order 10's of hours on 24 AMD Opteron 2.6 GHz cores, ~1 GB memory

Comparison to Experiment

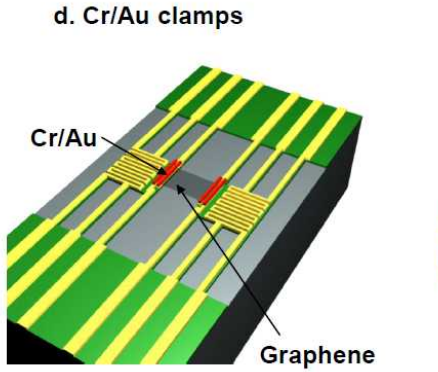

Xu, Y., Li, Z., and Duan, W., *Small* **10**, 2182 (2014).

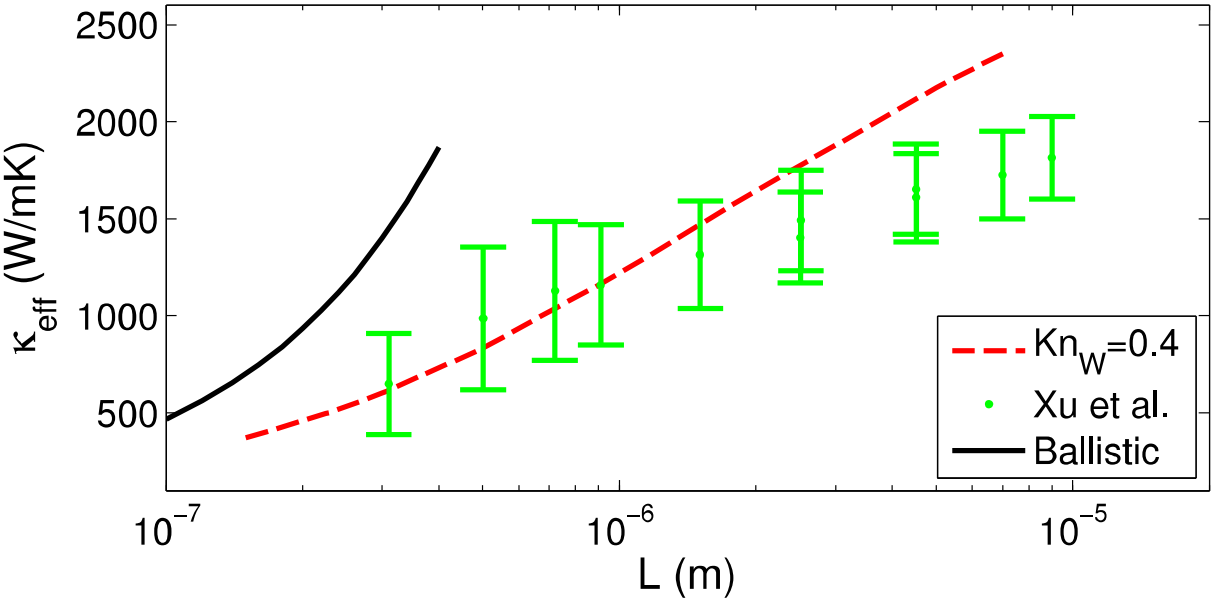

- Reasonable agreement with experiment
- Graphene ribbons 1.5 microns wide exhibit significant size effect

Conclusions

- We present an efficient method for solving spatially and time dependent phonon transport problems with the linearized three-phonon scattering operator.
- Classical size effects reduce thermal transport in graphene ribbons by 10-20\% for L, W of $\mathcal{O}(1\mu\mathrm{m})$.
- The homogenous scattering approximation over-predicts size effects by of 10-30% in the transition regime.
- Two dimensional size effects can be directly simulated

Acknowledgements

- Special thanks to Sangyeop Lee and Keivan Esfarjani for second and third order force constants from DFT/DFPT for graphene
- Financial Support from:
  - NSF Graduate Research Fellowship Program
  - NDSEG Fellowship
  - MIT-Singapore Alliance
- The author's ongoing research is funded by Sandia National Laboratories Laboratory Directed Research and Development Program. Sandia National Laboratories is a multiprogram laboratory managed and operated by Sandia Corporation, a wholly owned subsidiary of Lockheed Martin Corporation, for the U.S. Department of Energy's National Nuclear Security Administration under Contract DE-AC04-94AL85000.

Other work: TDTR

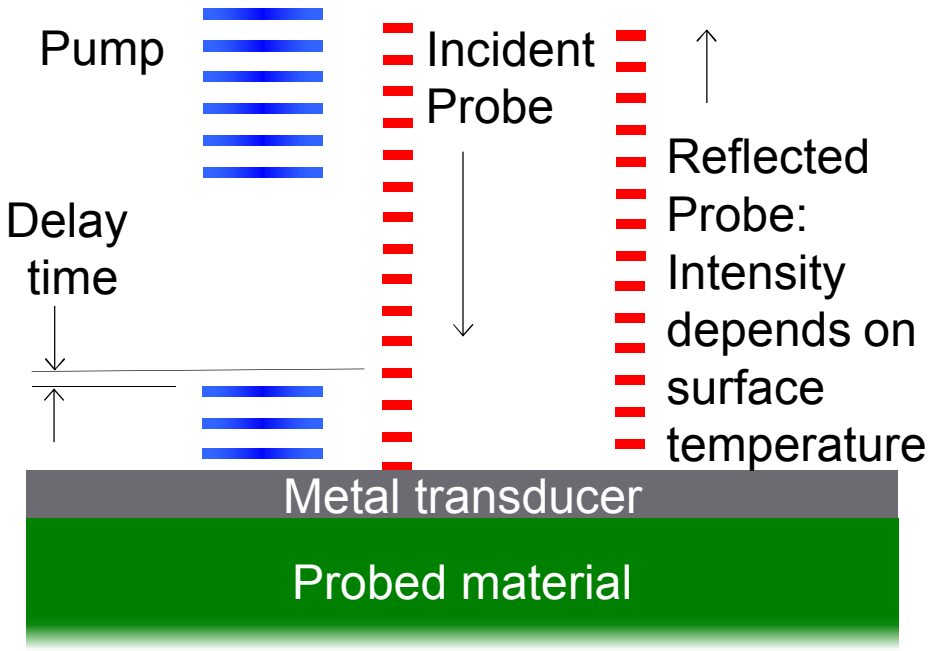

- 400nm pulses heat surface
- Reflectivity (temperature) probed by 800 nm pulse train
- Pump modulation varies heat pulse penetration depth

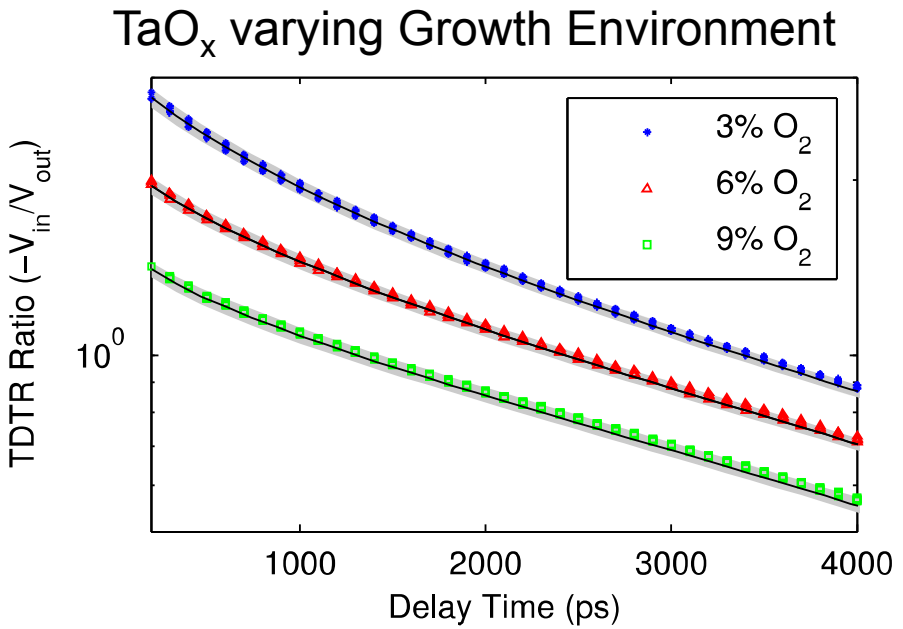

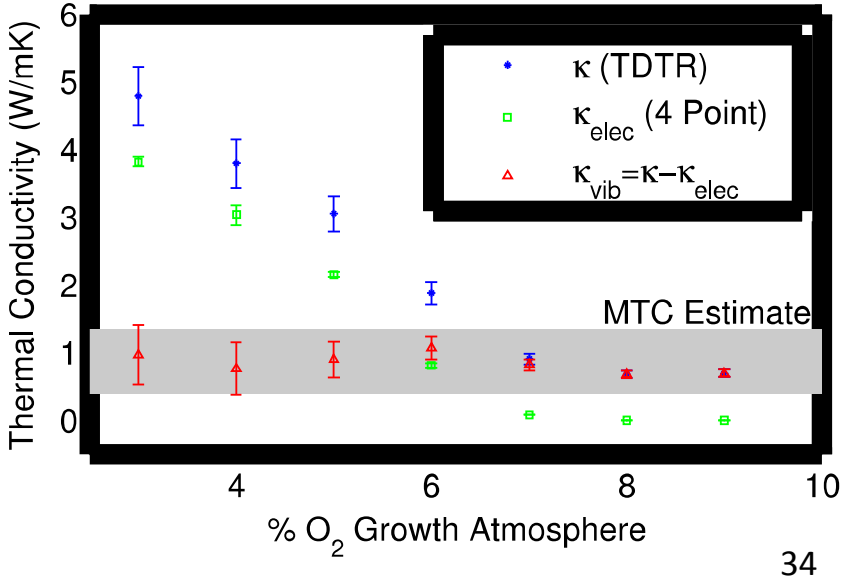

Other work: 2 D Materials

- Graphene Exfoliation
- Large area wet transfer of graphene
- Temperature dependent Raman spectroscopy of few layer materials
- Raman peak positions are sensitive to strain, temperature, and doping

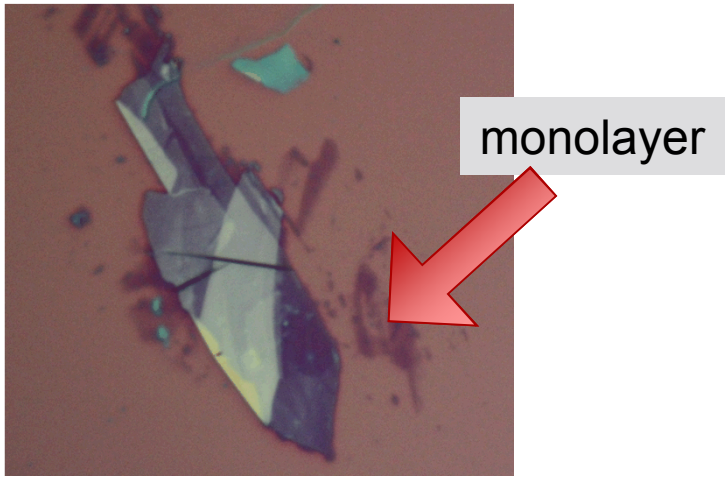

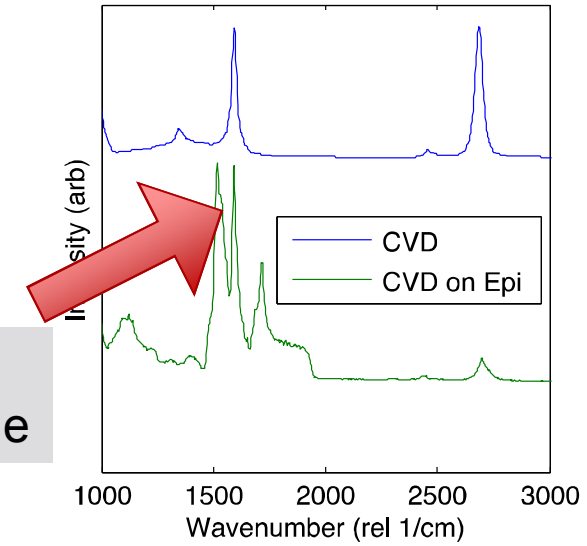

Resonant G peak in twisted bilayer graphene

Extra Slides

Sandia National Laboratories

A Few Words on Convergence

Sandia National Laboratories

- Convergence of homogeneous solution

TABLE II. Convergence of the iterative solution thermal conductivity with respect to discretization N_{side}.

N_{side}	$\kappa_{xx,\text{SMRT}}$	$\kappa_{yy,\text{SMRT}}$	κ_{xx}	κ_{yy}
5	586.18	579.74	1474.41	1434.02
11	468.97	481.62	2584.32	2533.65
21	510.51	530.40	3099.31	3013.94
31	515.51	535.35	3272.60	3160.60
41	513.87	533.38	3345.17	3237.89
51	515.01	534.18	3467.55	3336.47
61	514.84	533.81	3539.02	3397.62
71	514.42	533.30	3554.41	3401.23
81	513.13	531.91	3591.68	3444.19

- Convergence occurs more quickly for smaller structures
- Ratios converge by ~31 (e.g. $\kappa_{\text{eff}}/\kappa$)
- Time splitting converges as Δt,
- Time step: less than 1/3 cell traversal time
- Spatial convergence: preferably >10 cells per mean free path